THE JOURNAL OF PHYSICAL CHEMISTRY C

Article

pubs.acs.org/JPCC

Supercritical Deposition Route of Preparing Pt/Graphene Composites and Their Catalytic Performance toward Methanol Electrooxidation

Jian Zhao,*[,†,‡,§] Hui Yu,[†,‡] Zhensheng Liu,[†,‡] Min Ji,[†,‡] Liqing Zhang,[†,‡] and Guangwei Sun[§]

[†]Key Laboratory of Rubber-Plastics Ministry of Education/Shandong Provincial Key Laboratory of Rubber-Plastics, Qingdao University of Science & Technology, No. 53 Zhengzhou Road, Qingdao 266042, China

[‡]State Key Laboratory of Molecular Engineering of Polymers (Fudan University), Ministry of Education, Yuejin Building, No.220 Handan Road, Shanghai 200433, China

[§]Chongqing Key Laboratory of Micro/Nano Materials Engineering and Technology, No. 318 Honghe Road, Chongqing 402168, China

Supporting Information

ABSTRACT: The production of effective loading and direct deposition of Pt nanoparticles on graphene is difficult because this intriguing carbon material has highly hydrophobic surface properties. In this work, Pt/graphene sheet (GS) composites were successfully synthesized via a simple, effective, and environmentally benign one-pot supercritical carbon dioxide deposition route using dimethyl (1,5-cyclooctadiene) platinum(II) ($PtMe_2COD$) as a soluble organometallic precursor. The preparation process obviates the need for solvents, which are often volatile and toxic. No post-treatment processes such as washing and drying are needed. Transmission electron microscopy shows that ultrafine metal nanoparticles with an average size as small as ~2 nm are densely and evenly decorated on the hydrophobic surfaces of GS at Pt loadings up to 80 wt %. Electrochemical studies reveal that the prepared Pt/GS composites possess notably higher catalytic activity and better stability toward methanol electrooxidation in comparison with Pt/multiwalled carbon nanotube and Pt/carbon black composites. The supercritical carbon dioxide deposition method could be easily extended to the fabrication of other graphene-based metal composites with desirable properties by selecting suitable organometallic precursors.

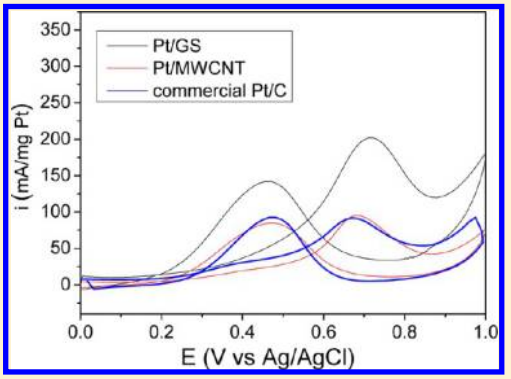

1. INTRODUCTION

Graphene, a single-atom-thick 2-D carbon material has fascinated academic and industrial communities owing to its unique structure, excellent chemical and physical properties, and its various potential applications in many technological fields such as nanoelectronics, sensors, nanocomposites, supercapacitors, batteries, and hydrogen storage.[1−7] In particular, graphene is expected to offer great advantages as a promising carbon-based support to immobilize noble metals for direct methanol fuel cell (DMFC) applications. As is well known, supporting materials are essential to electrocatalysts to achieve high catalytic activity for methanol electrooxidation because of their large effect on the particle size and distribution of the supported catalysts.[3] Carbon black (Vulcan XC-72) has been the most widely used electrocatalytic support in DMFCs.[8] In recent years, carbon nanotubes (CNTs) have also been extensively investigated as an excellent support and been demonstrated to effectively improve electrocatalytic activity of Pt or PtRu nanoparticles.[8−13] In comparison with rolled structured CNT, the advantages of graphene as a support lie in its high specific surface area (2600 m^2/g), high conductivity, potentially low manufacturing cost, and open structure with both sides that can be utilized to load nanoparticles.

The combination of graphene and Pt nanoparticles has demonstrated a robust strategy for catalyzing methanol electrooxidation. Until now, a number of methods for the synthesis of graphene/metallic nanoparticle composites have been developed successfully.[14−23] In typical fabrication processes, graphite oxide (GO) was employed as the starting material because, with the assistance of sonication or long-time stirring, the abundance of different oxygenated species on the surfaces of GO renders the solubilization of oxidized graphene sheets (GSs) in solvents and also allows metal precursors to intercalate into the interlayer space of GO. These oxygen-containing functional groups could provide nucleating sites for the growth of metal nanoparticle. To restore conductive sp^2-hybridized network of graphene, however, in situ or subsequent reduction of GO is needed, which requires complex manipulation and involves multiple steps. Besides, the

Received: March 15, 2013
Revised: October 30, 2013
Published: January 2, 2014

   dx.doi.org/10.1021/jp402620p | J. Phys. Chem. C 2014, 118, 1182−1190

developed methods suffer from the use of hazardous or toxic reducing agents, posing environmental and health risks.

Once the oxygen functionalities are absent from graphene, a homogeneous dispersion of Pt nanoparticles on GSs will be difficult. As reported by several research groups, the functionalization of GSs or the use of surfactants was required to stabilize GSs in solutions to uniformly load metal nanoparticles.[23−26] Unfortunately, the functionalization of graphene could negatively affect the intrinsic properties of graphene.[27] Recent investigations pose a highly important warning to the graphene community to always consider the effect/influence of any surfactant/solvent that is used to aid graphene dispersion because they have highly negative effects on the interpretation of electrochemical data.[28,29] The production of effective loading and direct deposition of metallic nanoparticles on GS remains challenging because of the hydrophobic nature of graphene. Therefore, it is urgently needed to find newly simple and clean synthesis routes to construct uniformly distributed graphene−metal nanoparticle hybrid.

In recent years, supercritical fluid (SCF) technology has been widely used to synthesize nanomaterials and nanocomposites due to the unique properties of SCF arising from the combination of a gas and a liquid. Low viscosity, rapid diffusion, the absence of surface tension, and the controllable solvent strength adjusted by changing fluid temperature and pressure make SCF easily deliver reactant molecules to areas with high aspect ratios and poorly wettable substrates. Among the SCFs, supercritical CO_2 (SC CO_2) (Tc = 31.1 °C, Pc = 71.8 bar) is particularly attractive for a wide variety of applications because it is chemically inert, nontoxic, inexpensive, environmentally acceptable, and leaves no residue in the treated medium. Such properties could be exploited in the development of novel processes for the synthesis of nanostructured materials. Lin and Erkey et al. reported that metal nanoparticles could be incorporated into different substrates via supercritical routes by the reduction of fluorinated or nonfluorinated organic precursors, respectively.[30,31] Recently, SC CO_2 were employed as an antisolvent to assist in the decoration of Pt or Pt Ru particles on graphene upon methanol or hydrogen reduction of inorganic or organic precursors.[32,33] It is remarkable that the use of organic solvents is needed and post-treatment such as tedious washing process is necessary in these preparation processes.

By utilizing supercritical carbon dioxide as a dissolving processing medium, we herein successfully demonstrate a facile, clean, and efficient one-pot SCF deposition route to disperse Pt nanoparticles on the hydrophobic surfaces of GS. No functionalization of graphene or employment of surfactants is involved in the preparation process. GSs used in this work were produced by rapid thermal expansion of GO. In the preparation process, dimethyl (1,5-cyclooctadiene) platinum(II) ($PtMe_2COD$) was dissolved in SC CO_2 and contacted with GS (without any pretreatment such as sonication), followed by thermal reduction under N_2 flow. Ultrafine platinum nanoparticles (∼2 nm) were deposited directly onto GSs at Pt loading up to 80 wt %. The Pt/GS composites removed from the stainless vessel is ready for use as an electrocatalyst immediately after the cessation of the thermal treatment. The electrocatalytic performance of the Pt/GS was investigated using methanol oxidation as the model system and compared with Pt/multiwalled carbon nanotube (MWCNT) and Pt/carbon black (C).

The use of CO_2 as the deposition medium and the soluble organic precursor obviates the need for solvents, which are often volatile and toxic. The thermal reduction of the precursor occurs at the graphene surface alone, thus excluding the particle formation in the fluid phase and subsequent precipitation of the particles onto the surface. As a result, the fabrication process results in uniformity in the particle size and stronger particle−support interaction, which are advantageous for enhanced electrocatalytic performance. Meanwhile, the volatilization of the nonfluorinated precursor ligands upon thermal treatment eliminates post-treatment processes such as washing and drying and also avoids emission problems (environmental concern).

Our investigation opens up a novel and insightful way to develop graphene-based electrocatalysts for fuel-cell applications, and the present method could be an interesting strategy extendable to synthesize other graphene-based metal composites by simply choosing suitable organometallic precursors.

2. EXPERIMENTAL SECTION

2.1. Materials. All of the chemicals used were of analytical grade, which were commercially obtained and used as received. Natural graphite powders (purity 99.99%, particle size 40 μm) were obtained from Qingdao Ruisheng Graphite. Carbon black (Vulcan XC-72, particle size, 30−100 nm; specific surface area, 150 m^2/g) was purchased from Cabot. MWCNTs (purity, >95%; diameter, 40−60 nm; length, 5−15 μm; special surface area, 300 m^2/g), prepared via catalytic decomposition of CH_4 using La_2NiO_4 as a catalyst precursor, were provided by Shenzhen Nanoport. MWCNTs were dispersed in 1 M HNO_3 solution for ∼6 h to remove the residual catalyst. This pretreatment method could not introduce oxygen-containing groups and has little influence on the structure of CNTs.[34] Dimethyl (1,5-cyclooctadiene) platinum(II) ($PtMe_2COD$, 97%) was purchased from Aldrich. CO_2 (99.999%) was provided by Qingdao Heli. Commercial Pt/C catalyst (20 wt % Pt) was purchased from Alfa Aesar.

2.2. Synthesis of Graphene Sheets. GSs were synthesized according to the previously described method.[35−37] 0.8g of GO (GO was prepared according to the method described by Hummers with some modifications[38,39]) was placed into a long quartz tube that was sealed at one end, and the other end was closed with a rubber stopper. Then, a nitrogen inlet was inserted through the rubber stopper. The sample was flushed with nitrogen for 5 min, and the quartz tube was quickly inserted into a muffle tube furnace preheated to 1050 °C and held in the furnace for 10 min under nitrogen flow. According to the investigation by Schniepp et al.,[36,37] the surface areas of dry GS powders determined by the Brunauer−Emmett−Teller (BET) method were in the range of 600−1500 m^2/g but still lower than the theoretical surface area of graphene because of the overlap of the exfoliated sheets.

2.3. Synthesis of Pt/GS, Pt/MWCNT, and Pt/C Composites. In a typical preparation procedure, 20 mg of GS and 40 mg of organometallic precursor $PtMe_2COD$ (in the case of 31 wt.% Pt/GS) were loaded into a high-pressure stainless vessel with a volume of 25 mL. (By varying the mass ratio of the organic precursor and GS, 60 and 80 wt % Pt/GS catalysts were also prepared.) The vessel was sealed and heated to 70 °C and then charged slowly with CO_2 to a pressure of 24.5 MPa using a syringe pump. The vessel was maintained at this temperature and pressure for ∼6 h, and then the vessel was depressurized. After the vessel was allowed to cool, the impregnated GS was weighed (the process is not necessarily

dx.doi.org/10.1021/jp402620p | J. Phys. Chem. C 2014, 118, 1182−1190

needed in the preparation process of Pt/GS) using an analytical balance accurate to ±0.1 mg to determine the amount of precursor adsorbed. Subsequently, the GS was heated in the vessel at 200 °C, and the precursor was heated under flowing N_2 for 4 h. Pt/MWCNT and Pt/C were also synthesized following a similar procedure. Although it is well known that MWCNTs produced by different methods (or from different providers) undergoing different pretreatment procedures would exhibit diverse properties, the MWCNTs we used have been reported to act as an excellent support for electrocatalysts.[12,13]

2.4. Characterization. XRD patterns were obtained using a D-MAX 2500/PC operated at 40 kV and 100 mA with Cu Kα radiation (λ = 0.15418 nm). The XPS measurement of the composites was performed on an RBD-upgraded PHI-5000C ESCA system (Perkin-Elmer) with Al Kα radiation ($h\nu$ = 1486.6 eV). The data analysis was carried out using RBD AugerScan 3.21 software (RBD Enterprises, USA). The morphology of the products was examined by TEM on a JEOL 2010 transmission electron microscope equipped with an energy-dispersive X-ray spectrometer (EDS). The samples were digested with 5 mL of HNO_3 and 5 mL of HCl in a hot block tube at 95 °C for 4 h. After being kept at room temperature overnight, 2 mL of HF was added to the sample solutions and digested at 95 °C for 2 h. The resulting solutions were analyzed by inductively coupled plasma spectroscopy/optical emission spectroscopy (ICP/OES, Perkin-Elmer, Optima 3300XL with AS 91autosampler) for the metal content of the prepared composites.

2.5. Electrochemical Measurements of the Composites. The electrochemical properties of the Pt/GS, Pt/MWCNT, and Pt/C composites were evaluated by cyclic voltammetry (CV) and chronoamperometry (CA) tests using a conventional three-electrode cell on a CHI660B electrochemical workstation (Chenhua, China). All tests were conducted at room temperature. A glassy carbon electrode coated with catalysts (3 mm in diameter) was used as the working electrode, a Pt wire as the counter electrode, and Ag/AgCl electrode as the reference electrode. 10 μL of *N*,*N*-dimethylformamide solution containing catalyst (2.5 mg/mL) was cast dropwise onto glass carbon electrode surface. After drying at room temperature in air, 8 μL of 0.05 wt % Nafion solution was dropped on the surface of the catalyst layer to form a thin film, protecting catalyst from detaching. Before the test, the working electrode was dried for 3 h at room temperature.

Electrochemically active surface area (ECSA) of Pt nanoparticles was calculated from the hydrogen electrosorption curve, which was recorded in 0.5 M H_2SO_4 solution. The electrocatalytic activity and stability of the synthesized Pt/GS, Pt/MWCNT and Pt/C for the oxidation of methanol were evaluated in 1 M CH_3OH and 0.5 M H_2SO_4 by means of CV and CA tests. The electrolyte solutions were deaerated with ultrahigh purity nitrogen for 15 min prior to any measurement.

3. RESULTS AND DISCUSSION

The XRD spectra of the GS and prepared Pt/GS (31 wt %) composites are shown in Figure 1. The pattern of Pt/GS contains several very broad peaks at the positions corresponding to the (1 1 1), (2 0 0), (2 2 0), and (3 1 1) planes of characteristic face-centered cubic (fcc) Pt lattice.[16,18] The broad peak at ~26° is assigned to the stacking structure of the GS (Figure 1b). Compared with the pristine GS in Figure 2a, an obvious decrease in the C(002) peak of Pt/GS (Figure.2b)

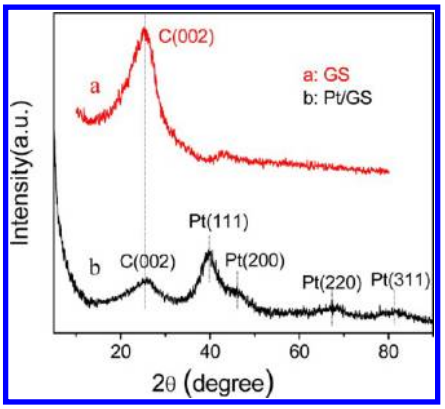

Figure 1. XRD patterns of (a) the GS and (b) the Pt/GS (31 wt %) composites.

reveals that the attached Pt nanoparticles can prevent GS from aggregating and restacking by functioning as a "spacer", thus making more surface area accessible.[40,41] As expected, no platinum oxide is detected by XRD analysis, indicating that the organometallic precursor ($PtMe_2COD$) absorbed on GS is mainly converted to zerovalent Pt.

The morphology of Pt/GS (31 wt %) is assessed by TEM. The typical TEM images of Pt/GS composites (Figure 2a) display a uniform distribution of ultrafine platinum nanoparticles on the wrinkled and nearly transparent GS, indicating a strong interaction between the graphene support and the Pt nanoparticles.[27,42] No agglomeration of metal nanoparticles is observed. The highly dispersed Pt nanoparticles on the large surface area of graphene are very favorable for reducing the use of the precious metal and maximizing its electrocatalytic activity.

The Pt nanoparticles on GS exhibit a particle size distribution in the range of 1.1 to 5.1 nm with a mean particle size of 2.23 nm (Figure S1a in the Supporting Information). This value is substantially smaller than the average size (3−5 nm) of Pt nanoparticles on graphene prepared by conventional solution methods.[18,20,43,44] Both sides of the GSs can be utilized for the decoration of Pt nanoparticles. The resultant composites were also characterized by EDS, and a typical spectrum is shown in Figure 2b. The EDS analysis further confirms the presence of Pt nanoparticles on GS.

The morphologies of Pt nanoparticles on the surfaces of MWCNTs and carbon black (Vulcan XC-72) are shown in Figure 2c,d. Much larger mean particle size (5.93 nm) and broader size distribution (2.1−17.5 nm, Figure S1b in the Supporting Information) are found in Pt/MWCNT, In the case of Pt/C, the average particle size is 2.88 nm and the size distribution is in the range of 1.2−5.9 nm (Figure S1c in the Supporting Information).

The metal content of the composites is estimated from the amount of the adsorbed precursor by an analytical balance accurate to ±0.1 mg. Two assumptions are made to calculate the content of Pt on the GS, MWCNT, and C.[30] First, all precursors adsorbed on the supports were fully converted to metal Pt without volatilization. Second, all precursor ligands were volatilized from the surface of the composites. The calculated values are 31.8 wt % for Pt/GS, 31.5 wt % for Pt/MWCNT, and 10.4 wt % for Pt/C, respectively. The metal contents were also evaluated using inductively coupled plasma/optical emission spectroscopy (ICP/OES) to check the validity of the calculated value. The platinum loading on graphene,

dx.doi.org/10.1021/jp402620p | J. Phys. Chem. C 2014, 118, 1182−1190

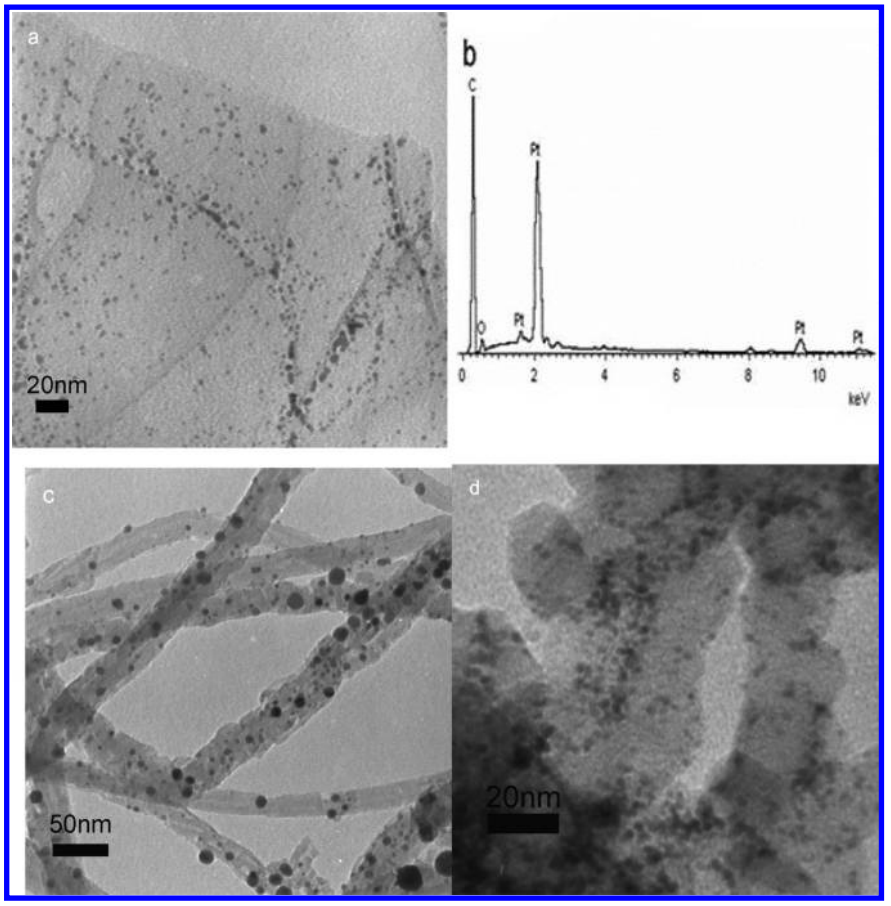

Figure 2. (a) TEM image of the Pt/GS (31 wt %) composites. (b) EDS spectrum of the Pt/GS (31 wt %) composites and the inset is the HRTEM image of Pt nanoparticle on GS. (c) TEM image of the Pt/MWCNT composites. (d) TEM image of the Pt/C composites.

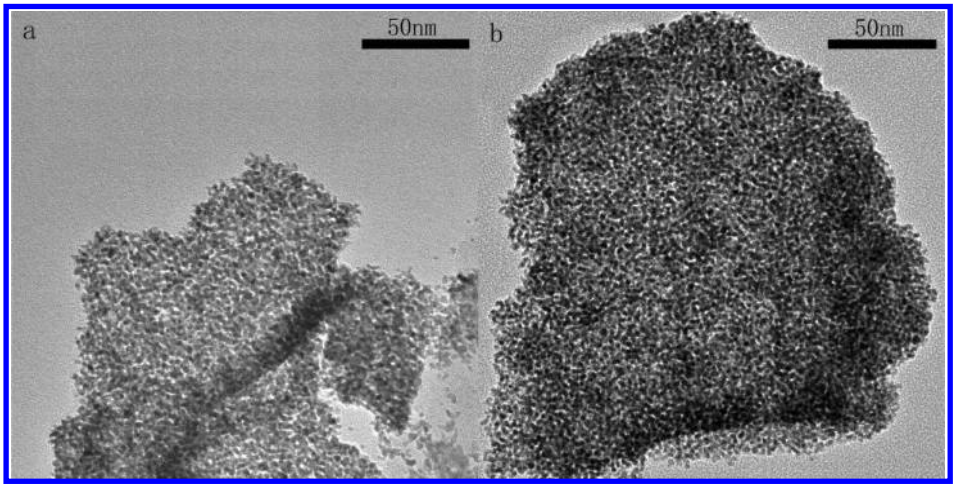

Figure 3. TEM images of (a) 60 and (b) 80 wt % Pt/GS composites.

MWCNT, and Vulcan is 31, 31, and 11 wt %, respectively, in agreement with the calculated Pt content.

The low Pt content on carbon black may be ascribed to its weaker affinity to the organometallic precursor, which leads to low absorption on carbon black. That is, the precursor has a more favorable affinity for graphene than for carbon black.[27,42,45] Despite their structural similarity of MWCNT and graphene, the platinum nanoparticles on MWCNT are larger and have broader size distributions than the Pt nanoparticles on graphene at similar metal content, which are associated with the relatively smaller surface area (compared with GS) and the relatively high metal content (compared with C).

By the use of this unique SCF method, the Pt loading density can be adjusted by simply varying the mass ratio of GS to the Pt organic precursor. TEM images of the Pt/GS catalyst reveal that the Pt nanoparticles are highly dispersed, even up to 80 wt % Pt/GS, as shown in Figure 3. Interestingly, the Pt particle size does not vary much with the increase in the Pt loading density. The mean sizes of Pt particles in the samples of 60 and

dx.doi.org/10.1021/jp402620p | J. Phys. Chem. C 2014, 118, 1182−1190

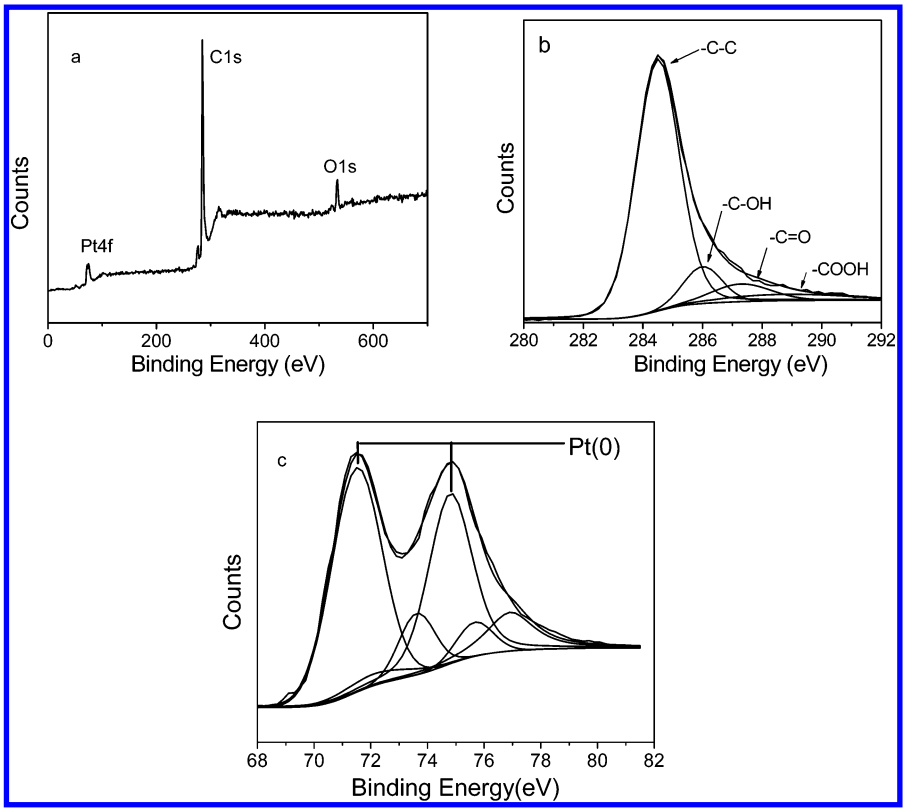

Figure 4. XPS spectra for the Pt/GS (31 wt %) composites: (a) survey spectrum of Pt/GS, (b) C1s spectrum of Pt/GS, and (c) Pt4f spectrum of Pt/GS.

80 wt % Pt/GS (the metal contents were determined using inductively coupled plasma/optical emission spectroscopy) were 2.32 and 2.46 nm, respectively. The relevant size distribution is shown in Figure S2 in the Supporting Information.

The homogeneous and dense distribution of Pt nanoparticles on GS could be attributed to the function of SC CO_2. The organometallic precursor ($PtMe_2COD$) can be dissolved in the solution of SC CO_2. Owing to the low viscosity, high diffusivity, and near-zero surface tension of the SCF, GS can be easily wetted by the precursor molecules. After depressurization, the impregnated organometallic precursor was adsorbed on the surfaces of GS, followed by nucleating on the surfaces of GS and growing into nanoparticles. The adsorbed precursor was converted to metal upon heat reduction. Meanwhile, the precursor ligands volatilized from the surfaces of the composites. The sizes and distributions of the Pt particles on graphene are uniform, suggesting that the precursor has a high affinity with graphene.[27,42] The utilization of SC CO_2 facilitates the formation of small, highly concentrated, and well-dispersed Pt nanoparticles on graphene. These results are significant because they not only show evenly distributed Pt nanoparticles but also obtain a high Pt loading on the hydrophobic surfaces of GS.

The low Pt content on carbon black makes the Pt/C composites prepared by this method not desirable for fuel-cell applications. We therefore make comparison with commercial Pt/C catalyst. The commercial catalyst (20 wt % Pt) was also characterized by TEM (Figure S3 in the Supporting Information). The average particle size (based on 200 nanoparticles) is 3.04 nm, and the size distribution of Pt nanoparticles on the carbon black is in the range of 0.9−5.7 nm. Compared with the commercial Pt/C catalyst, the Pt nanoparticles on the surface of GS exhibit the smaller average particle size (2.23 nm).

To investigate the covalent state of various species, XPS was carried out on the 31 wt % Pt/GS sample. Survey spectrum, C1s spectrum, and Pt4f spectrum of Pt/GS are shown in Figure 4. As shown in the survey XPS spectrum (Figure 4a), the presence of platinum is clearly observed, in good agreement with the EDS analysis. The C1s spectrum of Pt/GS is shown in Figure 4b. The high intensity of C−C bond (284.5 eV) indicates good sp^2 conjugation. The presence of a small amount of oxygen-containing groups such as −OH, −C═O, and −COOH on GS is detected, consistent with the investigation of Schniepp et al.[37] Strong doublet peaks at 71.5 (Pt $4f_{7/2}$) and 74.8 eV (Pt $4f_{5/2}$) are very similar to the values of Pt foil, indicating the existence of the element Pt.[46] The other two weaker doublets correspond to Pt oxides (Figure 4c).[47] The presence of Pt oxides could be attributed to the slight oxidation of nanoparticles upon exposure to air. The spectrum of Pt 4f suggests that most of Pt nanoparticles are zero-valence in Pt/GS.

As previously mentioned, the Pt/C catalyst fabricated by this SCF method shows a low Pt loading, which makes the Pt/C catalyst not favorable for DMFCs. (The relevant electrocatalytic tests of the prepared Pt/C catalyst are presented in Figure S4 in the Supporting Information.) We therefore selected the commercially available Pt/C catalyst as a control case to make a comparison and better evaluate the electrochemical performance of the graphene-supported Pt nanoparticles.

The electrochemical active surface areas (ECSAs) of the Pt/GS (31 wt.%), Pt/MWCNT, and commercial Pt/C electrodes are estimated from H_2 adsorption/desorption peaks using cyclic

dx.doi.org/10.1021/jp402620p | J. Phys. Chem. C 2014, 118, 1182−1190

voltammograms in 0.5 M H_2SO_4 solution (saturated with nitrogen) at 50 mV/s. The ECSA is an important parameter because it could not only provide information regarding the number of available electrochemically active sites but also be used to compare different electrocatalytic supports.[10,18,20] The well-defined hydrogen adsorption/desorption characteristics are shown in Figure 5. At negative potentials, typical hydrogen

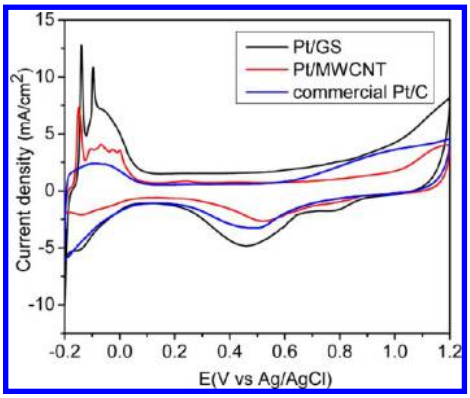

Figure 5. Cyclic voltammograms at the Pt/GS (31 wt %), Pt/MWCNT and commercial Pt/C electrodes in 0.5 M N_2-saturated H_2SO_4 solution at a scan rate of 50 mV/s.

adsorption and desorption peaks are observed, and characteristic peaks for the redox process of platinum are also formed at positive potential on Pt/GS, Pt/MWCNT, and commercial Pt/C. The ECSA can be determined by the integrated charge in the hydrogen region of the CVs. The calculation did not include the contribution of capacitive current.[48,49] The Pt/GS has much higher ECSA value (44.3 m^2/g) than Pt/MWCNT (32.8 m^2/g) and commercial Pt/C (30.1 m^2/g). This could be ascribed to the smaller size of the uniform ultrafine Pt nanoparticles on the huge surfaces of GS, which generates much more available active Pt sites for catalytic activity compared with Pt/MWCNT and commercial Pt/C.

Pt is considered to be one of the most promising candidates of metal catalysts for DMFC applications. Figure 6 compares CVs of the electrocatalytic methanol oxidation of Pt/GS, Pt/MWCNT, and commercial Pt/C, which were measured in 0.5 M H_2SO_4 solution containing 1 M CH_3OH. The stable voltammograms of the Pt/GS electrode were obtained after the 20th cycle. In the cases of the Pt/MWCNT and Pt/C catalysts, the voltammograms were obtained after the 20th and 15th

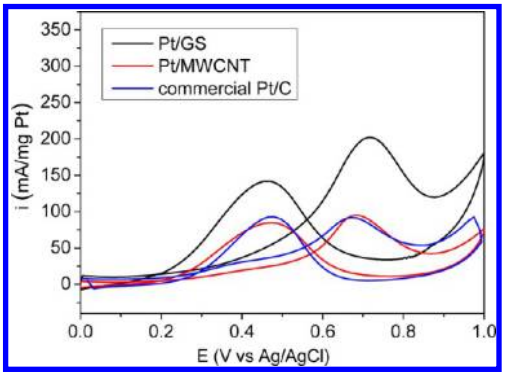

Figure 6. CVs of the Pt/GS (31 wt %), Pt/MWCNT and commercial Pt/C electrodes in the mixed solution of 1 M CH_3OH and 0.5 M H_2SO_4 at a scan rate of 20 mV/s.

cycles, respectively. During the whole process, oxidation peaks are found on the three electrodes. The forward oxidation current peak is attributed to the formation of CO_2 resulting from methanol oxidation, and the backward oxidation current peak is attributed to the removal of CO and other residual carbonaceous species resulting from incomplete methanol oxidation. Several critical parameters could be used to evaluate the catalytic activity of these carbon-based Pt electrodes: onset potential of methanol oxidation, forward oxidation peak current density, mass activity, and the ratio of the forward peak current density to the backward peak current density. The data are listed in Table 1.

It is demonstrated in Table 1 that the onset potential for methanol oxidation occurs at ~0.13 V on Pt/GS, which is more negative than that at 0.18 V on Pt/MWCNT and that at 0.20 V on commercial Pt/C. The lower onset potential of Pt/GS clearly shows that the Pt/GS electrode exhibits superior electrocatalytic performance toward methanol electrooxidation as compared with Pt/MWCNT and commercial Pt/C.

As can be seen from Figure 6, the mass activity of the Pt/GS catalyst is 202.2 mA per mg Pt, which is at least two times higher than those of the Pt/MWCNT and commercial Pt/C. The Pt nanoparticles on GS exhibit a much higher electrocatalytic activity for methanol oxidation in comparison with the Pt nanoparticles on MWCNT or on carbon black, consistent with the ECSA analysis. This high electrocatalytic activity of Pt/GS may be a result of the larger specific surface of graphene, the smaller size of the Pt nanoparticles, and unique graphitic basal plane structure of graphene. The ratio of the forward peak current density to the backward peak current density (I_f/I_b) can be used to evaluate the tolerance of catalysts toward the poisoning of intermediate species.[31] High I_f/I_b value indicates high tolerant ability to intermediate carbonaceous species. GS-supported Pt nanoparticles have a ratio of 1.43, higher than the values of Pt/MWCNT (1.13) and commercial Pt/C (0.99). This value is also higher than those of 3-D Pt-on-Pd bimetallic nanodendrites supported on graphene nanosheets (1.25)[26] and Pt/chemically converted graphene hybrid (0.83),[18] indicating that the Pt/GS prepared by the SCF method is much more tolerant to CO poisoning and methanol, can be oxidized to carbon dioxide much more efficiently.

Most of the previous studies for the GS-supported Pt catalysts have employed relatively low Pt loadings on the support (<50 wt % Pt). We herein also investigated the electrochemical performances of the highly concentrated Pt nanoparticles over GS (60 and 80 wt % Pt/GS). These Pt/GS catalysts show much higher mass activities (Figure 7) for methanol electrooxidation than the Pt/MWCNT and Pt/C catalysts (Table 1). In particular, the 60 wt % Pt/GS sample shows a mass activity (246.7 mA/mgPt) that is ~2.5 times higher than that of the commercial Pt/C catalyst. Among the Pt/GS composites, the 80 wt % Pt/GS sample exhibits the lowest mass activity (191.5 mA/mgPt) probably because the Pt nanoparticles for 80 wt % sample show more tendency to aggregate and have larger particle size.

The long-term cycle stabilities of the Pt/GS (31 wt %), Pt/MWCNT, and Pt/C catalysts for methanol oxidation were investigated in 1 M CH_3OH + 0.5 M H_2SO_4, aqueous solution by cycle voltammetry, and the corresponding results are shown in Figure 8.[50] In the case of Pt/GS, the peak current (converted to mass activity in Figure 8) remained almost constant from the 20th cycle to the 75th cycle after an initial increase. The peak current started to decrease gradually after the 75 cycles of

dx.doi.org/10.1021/jp402620p | J. Phys. Chem. C 2014, 118, 1182−1190

Table 1. Comparisons of Several Electrocatalytic Parameters for Pt/GS, Pt/MWCNT, and Pt/C

samples	onset potential (V)	ECSA (m^2/g)	I_f (mA/cm^2)	I_f/I_b	mass activity (mA/mg Pt)
Pt/C	0.18	17.4	4.1	1.35	96.9
Pt/MWCNT	0.18	32.8	10.4	1.13	95.5
Pt/GS (31 wt %)	0.13	44.3	22.1	1.43	202.2
commercial Pt/C	0.20	30.1	6.5	0.99	92.0

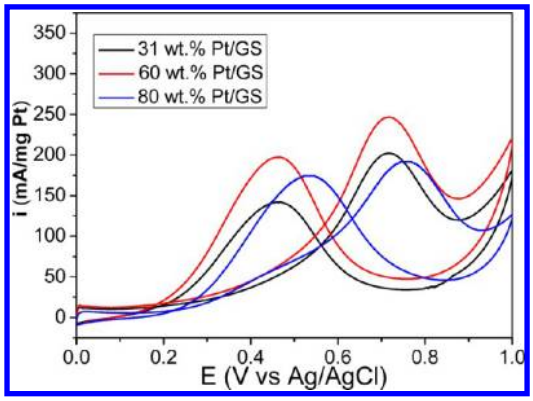

Figure 7. CVs of the Pt/GS catalysts with different amounts of Pt metal deposition, from 31 to 80 wt %, in the mix solution of 1 M CH_3OH and 0.5 M H_2SO_4 at a scan rate of 20 mV/s at room temperature.

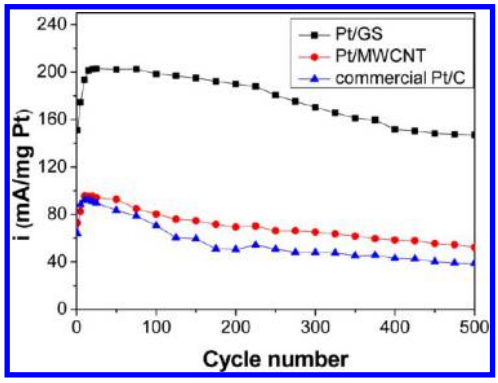

Figure 8. Long-term cycle stabilities of the Pt/GS (31 wt %), Pt/MWCNT, and commercial Pt/C electrodes in the mix solution of 1 M CH_3OH and 0.5 M H_2SO_4 at a scan rate of 50 mV/s.

potential scan. Using the peak current measured after the 20th cycle as the reference, the anodic peak current of the 500th cycle was ~73.2% of that measured at the 20th cycle. In the case of Pt/C, a poorer stability was observed. The peak current started to decrease quickly after 15 cycles. The peak current of the 500th cycle was 42.4% of that measured at the 15th cycle. In the case of Pt/MWCNT, the peak current started to decrease after 20 cycles. The peak current of the 500th cycle was 55.1% of the current density measured at the 20th cycle. The results imply that the Pt/GS catalyst possesses significantly improved long-term cycling stability for methanol oxidation as compared with the Pt/MWCNT and Pt/C catalysts.

Chronoamperometric experiments were also carried out to observe the stability of the catalysts under continuous operation. We have conducted chronoamperometry tests at 0.6 V for 20 min in a N_2 saturated solution of 0.5 M H_2SO_4 solution containing 1 M methanol. In the initial period, the current decay for all catalysts is observed due to the formation of the intermediate carbonaceous species for methanol oxidation (Figure 9). However, during the testing time, the

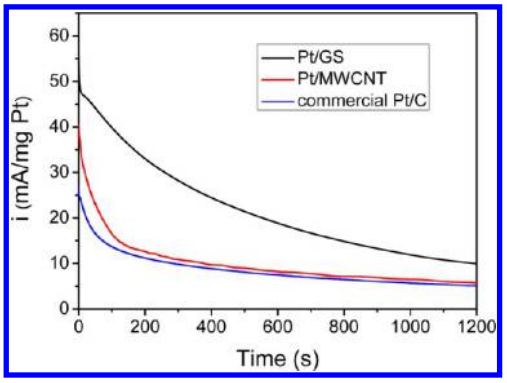

Figure 9. Current−time curves of Pt/GS (31 wt %), Pt/MWCNT, and commercial Pt/C electrodes at 0.6 V for 1200 s in the mix solution of 1 M CH_3OH and 0.5 M H_2SO_4.

current of methanol oxidation on Pt/GS is higher than those of Pt/MWCNT and commercial Pt/C. The result illustrates a higher catalytic activity and better stability for methanol oxidation in comparison with Pt/MWCNT and commercial Pt/C catalysts, in good agreement with the CV results. This 2D new carbon material is proved to be a better catalyst carrier.

By the means of supercritical carbon dioxide deposition, ultrafine Pt nanoparticles are well-dispersed on GSs and indeed improve the catalytic activity and stability for methanol oxidation. The large surface area of graphene and its high affinity with the organic precursor make this method particularly suited for the fabrication of graphene-based metal composites. The resulting Pt/GS composites with small particle size, excellent particle dispersion, and high metal content have a great prospect in fuel-cell applications.

4. CONCLUSIONS

We have demonstrated a facile, effective, and environmentally benign strategy to obtain highly dispersed Pt/graphene catalysts with a Pt particle size of ~2 nm using a supercritical deposition method (without the functionalization of graphene and the need of surfactants). The dense and homogeneous distribution of ultrafine Pt nanoparticles on the hydrophobic graphene surface is enabled by the utility of SC CO_2. No solvents are necessarily needed to enhance the solubility of the precursor in SC CO_2, and the prepared product is ready to use without any post-treatment. (No tedious washing process is involved to separate the product from the precursor.) By simply changing the mass ratio of the organic precursor and GSs, the loading of uniform Pt nanoparticles can be adjusted up to 80 wt % Pt loading. Remarkable enhancement of electrochemical performance for methanol oxidation is achieved in the Pt/GS composites as compared with its Pt/MWCNT and Pt/C counterparts. These results indicate that GSs could be an excellent candidate as a supporting material for electrocatalysts. The supercritical carbon dioxide deposition route could also be used to prepare other metal-based heterogeneous catalysts.

dx.doi.org/10.1021/jp402620p | J. Phys. Chem. C 2014, 118, 1182−1190

■ ASSOCIATED CONTENT

Supporting Information

Metallic nanoparticle size distribution of Pt/GS, metallic nanoparticle size distribution of Pt/MWCNT, and metallic nanoparticle size distribution of the prepared Pt/C. Metallic nanoparticle size distribution of 60 wt% Pt/GS and metallic nanoparticle size distribution of 80 wt% Pt/GS. TEM image of commercial Pt/C catalyst and metallic nanoparticle size distribution of commercial Pt/C catalyst. Cyclic voltammograms and current−time curve of the prepared Pt/C catalyst. This material is available free of charge via the Internet at http://pubs.acs.org.

■ AUTHOR INFORMATION

Corresponding Author

*Tel/Fax: +86 0532 84022725 E-mail: Jian.Zhao2010@gmail.com.

Notes

The authors declare no competing financial interest.

■ ACKNOWLEDGMENTS

The work was partially funded by the National Natural Science Foundation of China (nos. 51373088 and 51073082), the National Basic Research Program of China (No, 2012CB722606), the Scientific Research Foundation for the Returned Overseas Chinese Scholars, Qingdao Municipal Science and Technology Program, Basic Research Project(12-1-4-3-(7)-jch and 12-1-4-3-(25)-jch), Chongqing Key Laboratory of Micro/Nano Materials Engineering and Technology (open project KFJJ1202), MOE Key Laboratory of Organosilicon Chemistry and Material Technology of Ministry of Education (open project YJG2010-02) (Hangzhou Normal University), State Key Laboratory of Chemical Resource Engineering (open project CRE-2012-C-204) (Beijing University of Chemical Engineering), State Key Laboratory of Molecular Engineering of Polymers (open project K2013-20. Fudan University), and the natural science foundation of Shandong Province (ZR2012EMM003).

■ REFERENCES

(1) Rao, C. N. R.; Sood, A. K.; Subrahmanyam, K. S.; Govindaraj, A. Graphene: The New Two-Dimensional Nanomaterial. *Angew. Chem., Int. Ed.* **2009**, *48* (42), 7752−7777.

(2) Geim, A. K.; Novoselov, K. S. The Rise of Graphene. *Nat. Mater.* **2007**, *6* (3), 183−191.

(3) Stankovich, S.; Dikin, D. A.; Dommett, G. H. B.; Kohlhaas, K. M.; Zimney, E. J.; Stach, E. A.; Piner, R. D.; Nguyen, S. T.; Ruoff, R. S. Graphene-Based Composite Materials. *Nature* **2006**, *442* (7100), 282−286.

(4) Novoselov, K. S.; Jiang, D.; Schedin, F.; Booth, T. J.; Khotkevich, V. V.; Morozov, S. V.; Geim, A. K. Two-Dimensional Atomic Crystals. *Proc. Natl. Acad. Sci. U. S. A.* **2005**, *102* (30), 10451−10453.

(5) Novoselov, K. S.; Geim, A. K.; Morozov, S. V.; Jiang, D.; Katsnelson, M. I.; Grigorieva, I. V.; Dubonos, S. V.; Firsov, A. A. Two-Dimensional Gas of Massless Dirac Fermions in Graphene. *Nature* **2005**, *438* (7065), 197−200.

(6) Novoselov, K. S.; Geim, A. K.; Morozov, S. V.; Jiang, D.; Zhang, Y.; Dubonos, S. V.; Grigorieva, I. V.; Firsov, A. A. Electric Field Effect in Atomically Thin Carbon Films. *Science* **2004**, *306* (5696), 666−669.

(7) Huang, X.; Yin, Z.; Wu, S.; Qi, X.; He, Q.; Zhang, Q.; Yan, Q.; Boey, F.; Zhang, H. Graphene-Based Materials: Synthesis, Characterization, Properties, and Applications. *Small* **2011**, *7* (14), 1876−1902.

(8) Xu, W.; Lu, T.; Liu, C.; Xing, W. Nanostructured Ptru/C as Anode Catalysts Prepared in a Pseudomicroemulsion with Ionic Surfactant for Direct Methanol Fuel Cell. *J. Phys. Chem. B* **2005**, *109* (30), 14325−14330.

(9) Chien, C.; Jeng, K. Effective Preparation of Carbon Nanotube-Supported Pt−Ru Electrocatalysts. *Mater. Chem. Phys.* **2006**, *99*, 80−87.

(10) Kongkanand, A.; Vinodgopal, K.; Kuwabata, S.; Kamat, P. V. Highly Dispersed Pt Catalysts on Single-Walled Carbon Nanotubes and Their Role in Methanol Oxidation. *J. Phys. Chem. B* **2006**, *110* (33), 16185−16188.

(11) Tian, Z. Q.; Jiang, S. P.; Liang, Y. M.; Shen, P. K. Synthesis and Characterization of Platinum Catalysts on Multiwalled Carbon Nanotubes by Intermittent Microwave Irradiation for Fuel Cell Applications. *J. Phys. Chem. B* **2006**, *110* (11), 5343−5350.

(12) An, G.; Yu, P.; Mao, L.; Sun, Z.; Liu, Z.; Miao, S.; Miao, Z.; Ding, K. Synthesis of Ptru/Carbon Nanotube Composites in Supercritical Fluid and Their Application as an Electrocatalyst for Direct Methanol Fuel Cells. *Carbon* **2007**, *45* (3), 536−542.

(13) Zhao, Y.; Yang, X.; Zhan, L.; Ou, S.; Tian, J. High Electrocatalytic Activity of Ptru Nanoparticles Supported on Starch-Functionalized Multi-Walled Carbon Nanotubes for Ethanol Oxidation. *J. Mater. Chem.* **2011**, *21*, 4257−4263.

(14) Nethravathi, C.; Anumol, E. A.; Rajamathi, M.; Ravishankar, N. Highly Dispersed Ultrafine Pt and Ptru Nanoparticles on Graphene: Formation Mechanism and Electrocatalytic Activity. *Nanoscale* **2011**, *3* (2), 569−571.

(15) Shao, Y.; Zhang, S.; Wang, C.; Nie, Z.; Liu, J.; Wang, Y.; Lin, Y. Highly Durable Graphene Nanoplatelets Supported Pt Nanocatalysts for Oxygen Reduction. *J. Power Sources* **2010**, *195* (15), 4600−4605.

(16) Shafiei, M.; Spizzirri, P. G.; Arsat, R.; Yu, J.; du Plessis, J.; Dubin, S.; Kaner, R. B.; Kalantar-zadeh, K.; Wlodarski, W. Platinum/Graphene Nanosheet/Sic Contacts and Their Application for Hydrogen Gas Sensing. *J. Phys. Chem. C.* **2010**, *114* (32), 13796−13801.

(17) Liu, S.; Wang, J.; Zeng, J.; Ou, J.; Li, Z.; Liu, X.; Yang, S. "Green" Electrochemical Synthesis of Pt/Graphene Sheet Nanocomposite Film and Its Electrocatalytic Property. *J. Power Sources* **2010**, *195* (15), 4628−4633.

(18) Li, Y.; Gao, W.; Ci, L.; Wang, C.; Ajayan, P. M. Catalytic Performance of Pt Nanoparticles on Reduced Graphene Oxide for Methanol Electro-Oxidation. *Carbon* **2010**, *48* (4), 1124−1130.

(19) Yoo, E.; Okata, T.; Akita, T.; Kohyama, M.; Nakamura, J.; Honma, I. Enhanced Electrocatalytic Activity of Pt Subnanoclusters on Graphene Nanosheet Surface. *Nano Lett.* **2009**, *9* (6), 2255−2259.

(20) Seger, B.; Kamat, P. V. Electrocatalytically Active Graphene-Platinum Nanocomposites: Role of 2-D Carbon Support in Pem Fuel Cells. *J. Phys. Chem. C* **2009**, *113* (19), 7990−7995.

(21) Rochefort, A.; Yang, D. Q.; Sacher, E. Stabilization of Platinum Nanoparticles on Graphene by Non-Invasive Functionalization. *Carbon* **2009**, *47* (9), 2233−2238.

(22) Kou, R.; Shao, Y.; Wang, D.; Engelhard, M. H.; Kwak, J. H.; Wang, J.; Viswanathan, V. V.; Wang, C.; Lin, Y.; Wang, Y.; Aksay, I. A.; Liu, J. Enhanced Activity and Stability of Pt Catalysts on Functionalized Graphene Sheets for Electrocatalytic Oxygen Reduction. *Electrochem. Commun.* **2009**, *11* (5), 954−957.

(23) Si, Y.; Samulski, E. T. Exfoliated Graphene Separated by Platinum Nanoparticles. *Chem. Mater.* **2008**, *20* (21), 6792−6797.

(24) Si, Y.; Samulski, E. T. Synthesis of Water Soluble Graphene. *Nano Lett.* **2008**, *8* (6), 1679−1682.

(25) Li, Y.; Fan, X.; Qi, J.; Ji, J.; Wang, S.; Zhang, G.; Zhang, F. Gold Nanoparticles−Graphene Hybrids as Active Catalysts for Suzuki Reaction. *Mater. Res. Bull.* **2010**, *45* (10), 1413−1418.

(26) Guo, S.; Dong, S.; Wang, E. Three-Dimensional Pt-on-Pd Bimetallic Nanodendrites Supported on Graphene Nanosheet: Facile Synthesis and Used as an Advanced Nanoelectrocatalyst for Methanol Oxidation. *ACS Nano* **2009**, *4* (1), 547−555.

(27) Li, N.; Cao, M.; Hu, C. Review on the Latest Design of Graphene-Based Inorganic Materials. *Nanoscale* **2012**, *4* (20), 6205−6218.

(28) Brownson, D. A. C.; Kampouris, D. K.; Banks, C. E. Graphene Electrochemistry: Fundamental Concepts Through to Prominent Applications. *Chem. Soc. Rev.* **2012**, *41* (21), 6944−6976.
(29) Brownson, D. A. C.; Metters, J. P.; Kampouris, D. K.; Banks, C. E. Graphene Electrochemistry: Surfactants Inherent to Graphene Can Dramatically Effect Electrochemical Processes. *Electroanalysis* **2011**, *23* (4), 894−899.
(30) Zhang, Y.; Kang, D.; Saquing, C.; Aindow, M.; Erkey, C. Supported Platinum Nanoparticles by Supercritical Deposition. *Ind. Eng. Chem. Res.* **2005**, *44*, 4161−4164.
(31) Lin, Y.; Cui, X.; Yen, C. H.; Wai, C. M. Ptru/Carbon Nanotube Nanocomposite Synthesized in Supercritical Fluid: A Novel Electrocatalyst for Direct Methanol Fuel Cells. *Langmuir* **2005**, *21* (24), 11474−11479.
(32) Zhao, J.; Zhang, L.; Chen, T.; Yu, H.; Zhang, L.; Xue, H.; Hu, H. Supercritical Carbon-Dioxide-Assisted Deposition of Pt Nanoparticles on Graphene Sheets and Their Application as an Electrocatalyst for Direct Methanol Fuel Cells. *J. Phys. Chem. C* **2012**, *116* (40), 21374−21381.
(33) Zhao, J.; Zhang, L.; Xue, H.; Wang, Z.; Hu, H. Methanol Electrocatalytic Oxidation on Highly Dispersed Platinum−Ruthenium Graphene Catalysts Prepared in Supercritical Carbon Dioxide-Methanol Solution. *RSC Adv.* **2012**, *2*, 9651−9659.
(34) Liang, Q.; Liu, B.-C.; Tang, S.-H.; Li, Z.-J.; Li, Q.; Gao, L.-Z.; Zhang, B.-L.; Yu, Z.-L. Carbon Nanotubes Growth Catalyzed by La_2nio_4. *Acta. Chim. Sin.* **2000**, *58* (11), 1336.
(35) Hu, H.; Liu, Y.; Wang, Q.; Zhao, J.; Liang, Y. A Study on the Preparation of Highly Conductive Graphene. *Mater. Lett.* **2011**, *65* (17−18), 2582−2584.
(36) McAllister, M. J.; Li, J.; Adamson, D. H.; Schniepp, H. C.; Abdala, A. A.; Liu, J.; Herrera-Alonso, M.; Milius, D. L.; Car, R.; Prud'homme, R. K.; Aksay, I. A. Single Sheet Functionalized Graphene by Oxidation and Thermal Expansion of Graphite. *Chem. Mater.* **2007**, *19* (18), 4396−4404.
(37) Schniepp, H. C.; Li, J. L.; McAllister, M. J.; Sai, H.; Herrera-Alonso, M.; Adamson, D. H.; Prud'homme, R. K.; Car, R.; Saville, D. A.; Aksay, I. A. Functionalized Single Graphene Sheets Derived from Splitting Graphite Oxide. *J. Phys. Chem. B* **2006**, *110* (17), 8535−8539.
(38) Becerril, H. A.; Mao, J.; Liu, Z.; Stoltenberg, R. M.; Bao, Z.; Chen, Y. Evaluation of Solution-Processed Reduced Graphene Oxide Films as Transparent Conductors. *ACS Nano* **2008**, *2* (3), 463−470.
(39) Hummers, W. S.; Offeman, R. E. Preparation of Graphitic Oxide. *J. Am. Chem. Soc.* **1958**, *80* (6), 1339−1339.
(40) Xu, C.; Wu, X.; Zhu, J.; Wang, X. Synthesis of Amphiphilic Graphite Oxide. *Carbon* **2008**, *46* (2), 386−389.
(41) Cai, D.; Song, M. Preparation of Fully Exfoliated Graphite Oxide Nanoplatelets in Organic Solvents. *J. Mater. Chem.* **2007**, *17* (35), 3678−3680.
(42) Liu, J.; Zhou, H.; Wang, Q.; Zeng, F.; Kuang, Y. Reduced Graphene Oxide Supported Palladium−Silver Bimetallic Nanoparticles for Ethanol Electro-Oxidation in Alkaline Media. *J. Mater. Sci.* **2012**, *47* (5), 2188−2194.
(43) Xu, C.; Wang, X.; Zhu, J. Graphene−Metal Particle Nanocomposites. *J. Phys. Chem. C* **2008**, *112* (50), 19841−19845.
(44) Mu, Y.; Liang, H.; Hu, J.; Jiang, L.; Wan, L. Controllable Pt Nanoparticle Deposition on Carbon Nanotubes as an Anode Catalyst for Direct Methanol Fuel Cells. *J. Phys. Chem. B* **2005**, *109* (47), 22212−22216.
(45) Zang, J.; Wang, Y.; Bian, L.; Zhang, J.; Meng, F.; Zhao, Y.; Qu, X.; Ren, S. Bucky Diamond Produced by Annealing Nanodiamond as a Support of Pt Electrocatalyst for Methanol Electrooxidation. *Int. J. Hydrogen Energy* **2012**, *37* (8), 6349−6355.
(46) Bonet, F.; Delmas, V.; Grugeon, S.; Herrera Urbina, R.; Silvert, P. Y.; Tekaia-Elhsissen, K. Synthesis of Monodisperse Au, Pt, Pd, Ru and Ir Nanoparticles in Ethylene Glycol. *Nanostruct. Mater.* **1999**, *11* (8), 1277−1284.
(47) Frelink, T.; Visscher, W.; Cox, A.; Veen, J. Ellipsometry and Dems Study of the Electrooxidation of Methanol at Pt and Ru-Promoted and Sn-Promoted Pt. *Electrochim. Acta* **1995**, *40* (10), 1537−1543.
(48) Girishkumar, G.; Rettker, M.; Underhile, R.; Binz, D.; Vinodgopal, K.; McGinn, P.; Kamat, P. Single-Wall Carbon Nanotube-Based Proton Exchange Membrane Assembly for Hydrogen Fuel Cells. *Langmuir* **2005**, *21* (18), 8487−8494.
(49) Pozio, A.; De Francesco, M.; Cemmi, A.; Cardellini, F.; Giorgi, L. Comparison of High Surface Pt/C Catalysts by Cyclic Voltammetry. *J. Power Sources* **2002**, *105* (1), 13−19.
(50) Shang, N.; Papakonstantinou, P.; Wang, P.; Silva, S. R. P. Platinum Integrated Graphene for Methanol Fuel Cells. *J. Phys. Chem. C* **2010**, *114* (37), 15837−15841.